Analysis of mulched drip irrigation with brackish water in cotton fields using the HYDRUS-3D numerical model

Authors: Yuyang, Shan, Lijun, Su, Quanjiu, Wang, Yan, Sun, Weiyi, Mu, et al.

Source: Canadian Journal of Soil Science, 102(4) : 959-976

Published By: Canadian Science Publishing

URL: https://doi.org/10.1139/cjss-2022-0047

Canadian Journal of Soil Science

Article

Analysis of mulched drip irrigation with brackish water in cotton fields using the HYDRUS-3D numerical model

Shan Yuyang, Su Lijun, Wang Quanjiu, Sun Yan, Mu Weiyi, Zhang Jihong, and Wei Kai

State Key Laboratory of Eco-hydraulics in Northwest Arid Region of China, Xi'an University of Technology, Xi'an 710048, China

Corresponding author: **Su Lijun** (email: sljun11@163.com)

Abstract

This study combined continuous monitoring in the field using computer modeling to understand soil water movement and salt transport so as to design a suitable irrigation system for cotton using mulched drip irrigation with brackish water. A reasonable irrigation regime was determined and verified using thresholds of water and salinity stress in the various stages of cotton growth. In addition, some key factors, such as emitter discharge rate, emitter spacing, and initial water content, were screened for simulation, and irrigation uniformity and desalination rate were selected as the indicators for evaluation. The results showed that: (*i*) The HYDRUS-3D model was a useful tool for designing suitable irrigation regimes, and the determined suitable irrigation quota was 5160 m^3 hm^{-2} under mulched drip irrigation with brackish water during the growth period of cotton in 2019. (*ii*) The irrigation uniformity and leaching rate decreased with an increase in the emitter discharge, and the linear relationship between uniformity, leaching rate, and emitter discharge could be identified. (*iii*) The irrigation uniformity and leaching rate decreased with an increase in emitter spacing, and power functions might be used to calculate uniformity, leaching rate, and emitter spacing. (*iv*) The irrigation uniformity and leaching rate increased with an increase in initial water content, and the relationship between the two indexes and initial water content was defined by a linear function and a power function, respectively. These results provided a valuable reference for the rational use of drip irrigation with brackish water.

Key words: brackish water, mulched drip irrigation, cotton agriculture, HYDRUS model, suitable irrigation volume

Résumé

La présente étude combinait la surveillance continue sur le terrain et la modélisation sur ordinateur en vue de mieux comprendre les déplacements de l'eau et le transport du sel dans le sol, et ainsi concevoir un système d'irrigation au goutte-à-goutte utilisant de l'eau saumâtre qui conviendrait à la culture du coton sur paillis. Les auteurs ont établi un régime d'irrigation raisonnable puis l'ont vérifié avec le seuil de tolérance au stress hydrique et le stress causé par la salinité à divers stades de croissance de la plante. Parallèlement, ils ont contrôlé quelques paramètres importants comme le débit de sortie du goutteur, l'espacement des goutteurs ainsi que la teneur en eau initiale du sol. L'uniformité de l'irrigation et le taux de dessalement ont été retenus comme indicateurs pour l'évaluation. Les résultats de l'étude sont les suivants. (*i*) Le modèle 3D HYDRUS s'avère un outil utile pour créer un programme d'irrigation adéquat et, en 2019, le taux d'irrigation avec de l'eau saumâtre qui convenait à la croissance du coton sur paillis se situait à 5 160 m^3 par cent mètres carrés. (*ii*) L'uniformité de l'irrigation et le taux de lixiviation diminuent quand le débit du goutteur augmente et les auteurs ont établi un lien linaire entre ces trois paramètres. (*iii*) L'uniformité de l'irrigation et le taux de lixiviation diminuent avec un plus grand écartement des goutteurs et on peut se servir des fonctions de puissance pour calculer l'uniformité de l'irrigation, le taux de lixiviation ainsi que l'écartement des goutteurs. (*iv*) L'uniformité de l'irrigation et le taux de lixiviation augmentent avec la teneur en eau initiale du sol et une fonction linéaire ou de puissance définit respectivement les liens entre chaque indicateur et la concentration d'eau au départ. Ces résultats s'avéreront de précieuses références en vue d'un usage rationnel de l'irrigation au goutte-à-goutte avec de l'eau saumâtre. [Traduit par la Rédaction]

Mots-clés : eau saumâtre, irrigation au goutte-à-goutte sur paillis, culture du coton, modèle HYDRUS, débit convenant à l'irrigation

1. Introduction

According to the Food and Agriculture Organization, the world population will reach 9 billion by 2050 (Stein et al. 2020). Hence, it is necessary to increase production in agriculture to meet the required food demand (Foley et al. 2011). However, achieving this goal poses significant challenges with the increasing shortage of freshwater resources. In the last few decades, many studies have shown that the use of

brackish water (i.e., water with a salinity of 2–5 g L^{-1} (MWR 1998)) for agricultural irrigation does not always reduce crop yields, but can also improve crop quality (Mizrahi et al. 1988; Del et al. 2001; Bustan et al. 2005; Chen et al. 2009; Kang et al. 2010; Wan et al. 2010; Yang et al. 2020). However, studies have found that the use of brackish water can lead to a decline in crop yields and adversely affect soil quality (Bustana et al. 2004; Li et al. 2015; Chamekh et al. 2016; Cuccia et al. 2019). Hence, the use of brackish water for farmland irrigation requires careful consideration of various factors such as regional characteristics, irrigation methods and schedules, nature of crops grown, and so on.

Xinjiang is a typical arid-semiarid region in northwest China, and the largest cotton producer in the country. Maintaining cotton production is a challenge due to freshwater resource scarcity in the region, coupled with an increase in the area of cotton planting. Therefore, alternative water supplies need to be exploited urgently. Owing to the high evaporation rates and brackish water characteristics in Xinjiang, using brackish water with drip irrigation methods under mulch can effectively solve the problem of water shortage and ensure cotton yield (Che et al. 2021). However, some studies have suggested that the soil quality, and cotton growth and yield can be adversely affected by irrigation using brackish water (Chen et al. 2020). Therefore, suitable drip irrigation schedules need to be designed and relevant key factors need to be fully considered. These factors include knowledge of water movements, technical parameters, such as emitter spacing and emitter discharge, and crop types and characteristics.

Many experiments have been carried out to fully understand water movement and salinity transport when brackish water is used in drip irrigation schemes, besides experiments to understand suitable environments for cotton in different growth stages. For example, Yang et al. (2020) found that cotton yield was not seriously affected when using brackish water with salinity <6 g L^{-1}, although more than 6 g L^{-1} could inhibit root water uptake and result in yield loss. Chen (2010) examined cotton salinity stress drip irrigation with brackish water in various growth stages and obtained various salinity threshold values including 6.9 g kg^{-1}, 8.2 g kg^{-1}, and 9.2 g kg^{-1} in the bud stage, flower stage, and boll stage, respectively.

In addition to field experiments, many numerical models have been used to evaluate the movement of water and soil salinity under conditions involving brackish water irrigation or saline shallow water tables. Compared with field experiments, mathematical models have the advantage of saving time, expense, and labor. The models used include HYDRUS (Šimůnek et al. 2016; Zhang et al. 2021), SWAP (Yuan et al. 2019), LEACHC (Ali and Elliott 2000), SALTMED (Karandish and Šimůnek 2019), and UNSATCHEM (Rasouli et al. 2013). The HYDRUS model can simulate water movement and solute transport in two and three dimensions, and can flexibly accommodate various types of boundary conditions. Hence, it has been widely used to simulate soil water and salinity distributions under brackish water irrigation and optimize water management strategies. Wang et al. (2012) employed the HYDRUS model to simulate water and salinity distributions during the different growth stages of cotton and suggested optimum irrigation volumes.

However, current irrigation strategies still have some issues and, hence, need to be improved. Most of the studies to date used either planar or axi-symmetrical two-dimensional models to simulate water movement with drip irrigation (Karandish and Šimůnek 2018; Ghazouani et al. 2019; Nazari et al. 2020; Shiri et al. 2020). Drip irrigation presents a fully three-dimensional flow problem, especially when two adjacent wetting patterns begin to overlap (Kandelous et al. 2011) because the confluence of wetting fronts is common, and cotton is often planted in overlap zones (i.e., the zone irrigated by both adjacent drippers). Hence, knowledge of the distributions of water and salinity in overlap zones is highly important for achieving high crop yields. For cotton, water stress and salinity stress thresholds change with the growth stage, but the designs of irrigation volumes rarely consider threshold change over time, which may lead to too much or too little soil water, soil accumulation or leaching rates not being satisfactory, and cotton suffering from water and salinity stress.

Taking the aforementioned factors into consideration, we decided to employ the HYDRUS (2D/3D) software to study the optimal irrigation mode of cotton under film drip irrigation with brackish water, with the main objectives being (*i*) to calibrate and validate the HYDRUS (2D/3D) model for drip irrigation with brackish water, (*ii*) to evaluate soil salinity spatial-temporal dynamics, and (*iii*) to optimize the irrigation volume in different growth stages. The study aimed to provide a basis for the better use of drip irrigation with brackish water and, hence, deliver an optimum environment for cotton growth.

2. Materials and methods

2.1. Study site

Field experiments were conducted in 2018 and 2019 at the Management of Irrigation Station of BaZhou District in Korla County, China (41°35′N, 86°10′E, 911 m a.s.l.). The region is classified as a warm-temperate arid zone with a continental climate. The annual precipitation is 53.5–62.7 mm; the annual average evaporation is 2273–2788 mm; the total annual sunshine duration is 3036 h and the groundwater level is 5–6 m. The soil type is classified as loamy, with a mean soil bulk density of 1.51 g cm^{-3}. The average soil salinity content is 7.5 g kg^{-1} and the soil field capacity is 0.243 cm^3 cm^{-3}.

The initial soil salinity was 7.63 g kg^{-1} and 7.42 g kg^{-1} in 2018 and 2019, respectively, and the mean groundwater table depth during the crop growth seasons was 6.3 and 5.8 m in 2018 and 2019, respectively.

2.2. Drip irrigation system: Irrigation and fertilization schedules

Each plot was 13.5 m × 10 m and adjacent plots were separated by 1 m to eliminate the effect of the lateral movement of soil water. The planting pattern and drip line arrangement in the field followed the local practice of “one

Fig. 1. Planting and drip-line arrangements in the experimental plot. [Color online.]

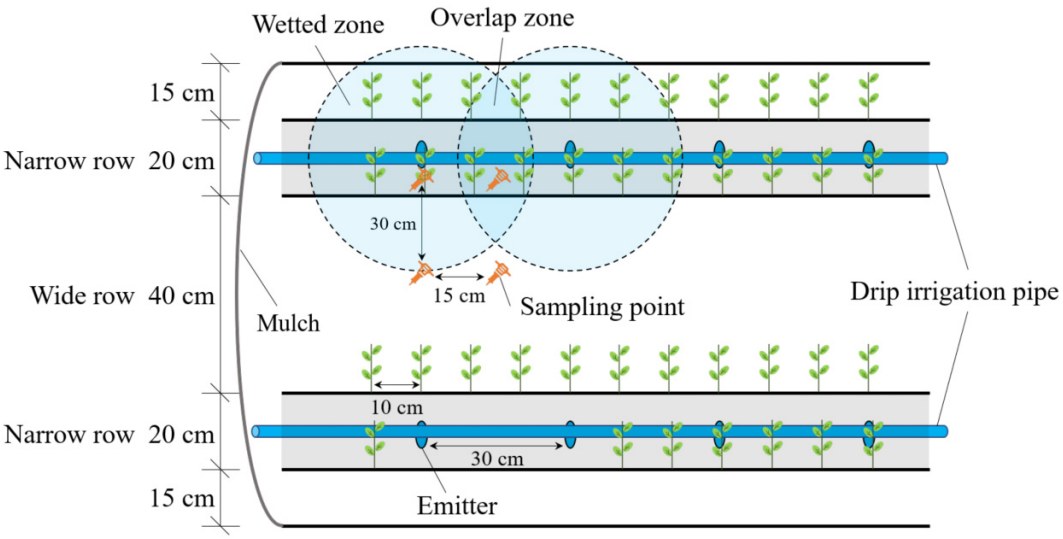

Table 1. Irrigation schedules applied in 2018 and 2019.

Year	Stage	Bud stage			Flower stage			Bell stage					Boll stage
2018	Irrigations times	3			3			5					1
	Irrigation cycles (days cycles^{-1})						7						
	Irrigation quota (m^3 hm^{-2})	300	300	375	375	375	450	450	450	525	525	450	300
	Total applied volume (m^3 hm^{-2})						4875						
2019	Irrigations times	3			3			5					1
	Irrigation cycles (days cycles^{-1})						7						
	Irrigation quota (m^3 hm^{-2})	450	450	450	405	405	405	450	450	450	450	450	300
	Total applied volume (m^3 hm^{-2})						5160						

film, two drip lines, and four rows" (Fig. 1). Four rows of cotton were covered by one white plastic film of 110 cm in width and irrigated with two drip lines with emitter intervals of 30 cm and an emitter discharge rate of 1.8 L h^{-1}. The width of the bare strip between a pair of mulches was 30 cm. The irrigation regimes during both growing seasons (2018 and 2019) are given in Table 1. The field was irrigated 12 times a year. The total amounts of applied water was 4875 m^3 h m^{-2} and 5160 m^3 h m^{-2} in 2018 and 2019, respectively. The irrigation water was extracted from groundwater with a salinity of 2.8 g L^{-1} and 2.4 g L^{-1} in 2018 and 2019, respectively.

A compound fertilizer, consisting of urea 375 kg hm^{-2}, ammonium phosphate 300 kg hm^{-2}, potassium sulfate 300 kg hm^{-2}, and farm manure 225 kg hm^{-2}, was applied to the soil before planting. The fertilizer was also applied during cotton growth every two irrigation cycles (every 7 days) at a rate of urea 45 kg hm^{-2} between bud and the start of bolling and urea 75 kg hm^{-2} thereafter to the bolling peak.

2.3. Samples collected and tested

The soil samples were collected from four depth layers (0–10, 10–20, 20–30, and 30–40 cm) at four locations (0 and 30 cm from an emitter, in the center of the overlap region between two emitters, and 30 cm from the center of the overlap region) randomly located within a treatment plot in the cotton budding stage, flowering stage, bell stage, and bolling stage. The soil samples were weighed, dried in a fan-assisted oven at 105 ± 2 °C for 24 h, and reweighed to determine the gravimetric soil water content (SWC). Volumetric SWC was then obtained by multiplying the gravimetric SWC with the average soil bulk density.

The electrical conductivity (EC) of soil-solution extracts (1:5 soil:water) was measured with a DDS-307 A conductivity meter (Shanghai Precision & Scientific Instrument Inc., Shanghai, China). The salinity thresholds were usually expressed in g kg^{-1} in China. Therefore, the relationship between g kg^{-1} and dS m^{-1} was determined as follows. A 1:5 soil:water mixture was shaken for 3 min and filtered. Then, 60 mL of the filtrate was placed in a porcelain dish and heated in a water bath. It was then oven-dried in the dish for 4 h, cooled for 30 min, and weighed. The filtrate was dried for a further 2 h and reweighed, checking that the two measurements were equal. The solid residue was then mixed with 15% hydrogen peroxide and heated in a water bath, and the other operations were repeated. The relationship between S and EC was then found to be

$$S = 4.02 \times EC_{1:5} \quad R^2 = 0.989 \tag{1}$$

Table 2. Estimated soil hydraulic parameters.

θ_r (cm^3 cm^{-3})	θ_s (cm^3 cm^{-3})	α (cm^{-1})	n	K_s (cm day^{-1})	l	D_L (cm)	D_T (cm)
0.058	0.42	0.036	1.6	38.3	0.5	55	40

Fig. 2. Comparison of observed and simulated soil water content (a) and salinities (b) in the cotton seedling stage. N, narrow stripe; W, wide stripe. [Color online.]

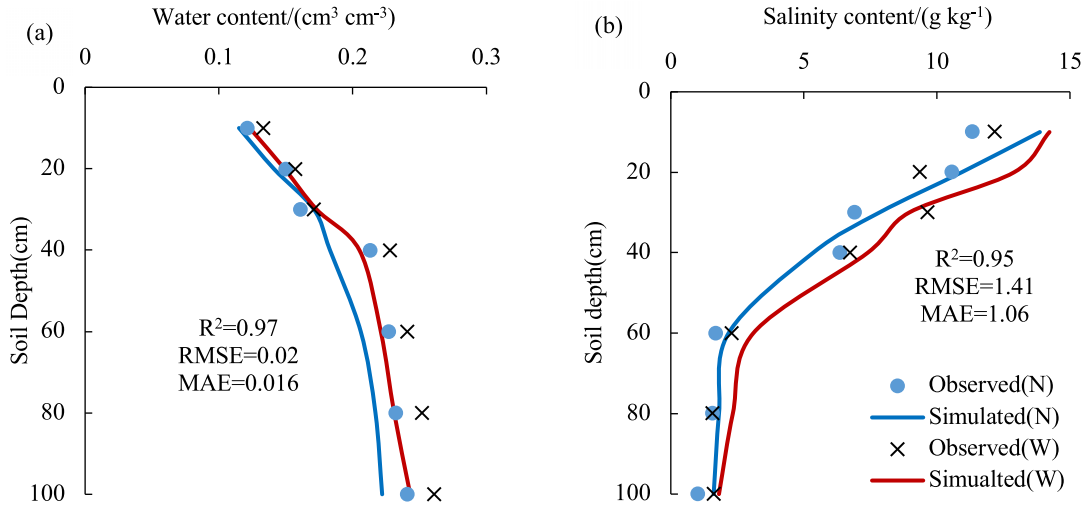

Fig. 3. Comparison of observed and simulated soil water content (a) and salinities (b) in the cotton boll stage. N, narrow stripe; W, wide stripe. [Colour online.]

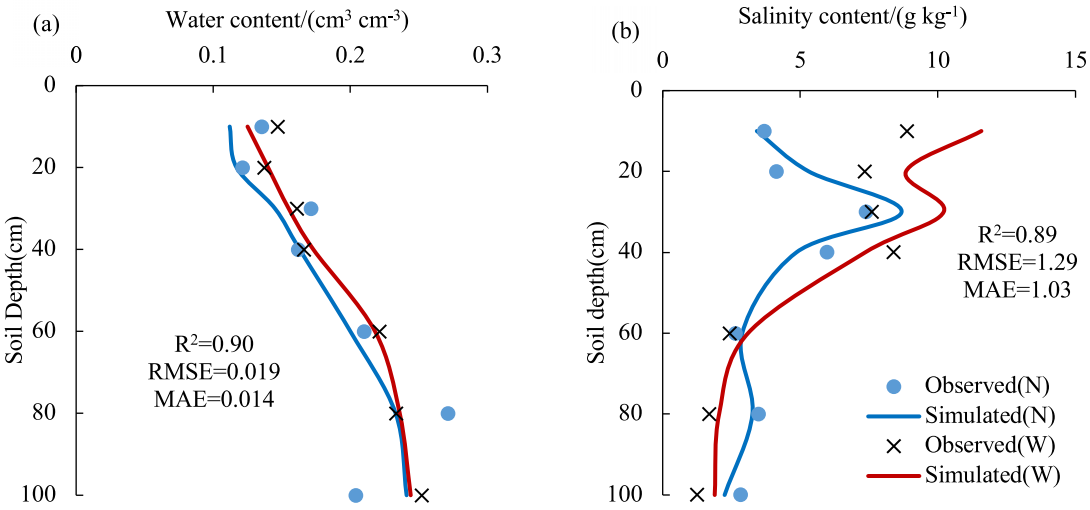

where S is the salinity (g kg^{-1}) and $EC_{1:5}$ is the measured conductivity (dS m^{-1}).

2.4. Numerical modeling

2.4.1. Water-flow simulation

The equation governing flow for the experimental conditions was given by the following modified form of Richards' equation:

$$(2)\quad \frac{\partial\theta}{\partial t} = \frac{\partial}{\partial x_i}\left[K\left(K_{ij}^A\frac{\partial h}{\partial x_j} + K_{iz}^A\right)\right] - S$$

where θ is the volumetric water content (cm^3 cm^{-3}), h is the pressure head (cm), t is time (min), x_i (i = 1, 2, 3 for a three-dimensional model) are spatial coordinates (cm), S is the sink term (cm^3 cm^{-3} min^{-1}), K_{ij}^A and K_{iz}^A are components of the dimensionless anisotropy hydraulic K^A (dimensionless), and K is

Fig. 4. Soil water content at different positions during the four cotton growth stages in the 2 years, 2018(a) and 2019(b). N, narrow stripe; W, wide stripe; O, overlap zone. [Color online.]

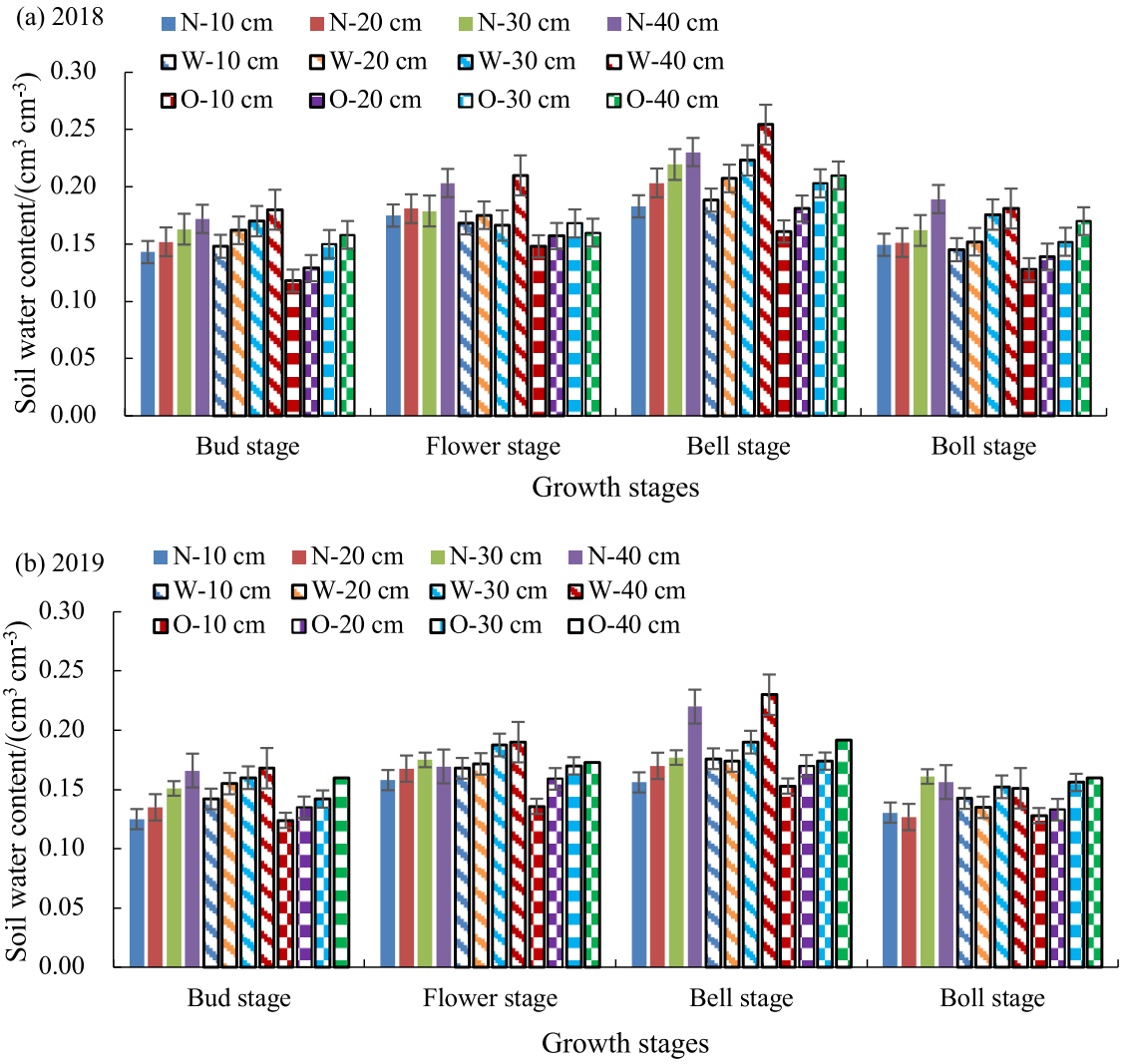

the unsaturated hydraulic-conductivity function (cm min^{-1}) given by conductivity tensor:

$$K(h,x,y,z) = K_s(x,y,z)\,K_r(h,x,y,z) \quad (3)$$

where K_r is the relative hydraulic conductivity (dimensionless) and K_s is the saturated hydraulic conductivity (cm min^{-1}).

The soil hydraulic properties were specified based on the van Genuchten model:

$$\theta(h) = \begin{cases} \theta_r + \dfrac{(\theta_s - \theta_r)}{\left(1 + |\alpha h|^n\right)^m} & h < 0 \\ \theta_s & h \geq 0 \end{cases} \quad (4)$$

$$K(h) = \begin{cases} K_s S_e \left[1 - \left(1 - S_e^{1/m}\right)^m\right]^2 & h < 0 \\ K_s & h \geq 0 \end{cases} \quad (5)$$

$$S_e = \frac{\theta - \theta_r}{\theta_s - \theta_r} \quad (6)$$

where θ_s is the saturated water content (cm^3 cm^{-3}); θ_r is the residual water content (cm^3 cm^{-3}); α, n, and l are shape parameters, with $m = 1–1/n$; and S_e is the effective saturation.

2.4.2. Salt-transport simulation

Solute transport within the soil profile, which is controlled by both infiltration and diffusion, could be described by the advection–diffusion equation (eq. 7):

$$\theta \frac{\partial c}{\partial t} = \frac{\partial}{\partial x_i}\left(\theta D_{ij}^w \frac{\partial c}{\partial x_j}\right) - \frac{\partial q_i c}{\partial x_i} \quad (7)$$

where c is the solute concentration in the liquid (g L^{-1}), D_{ij}^W is the effective dispersion coefficient tensor in the soil

Fig. 5. Soil salinity at different positions during the four cotton growth stages in the 2 years, 2018(a) and 2019(b). N, narrow stripe; W, wide stripe; O, overlap zone. [Color online.]

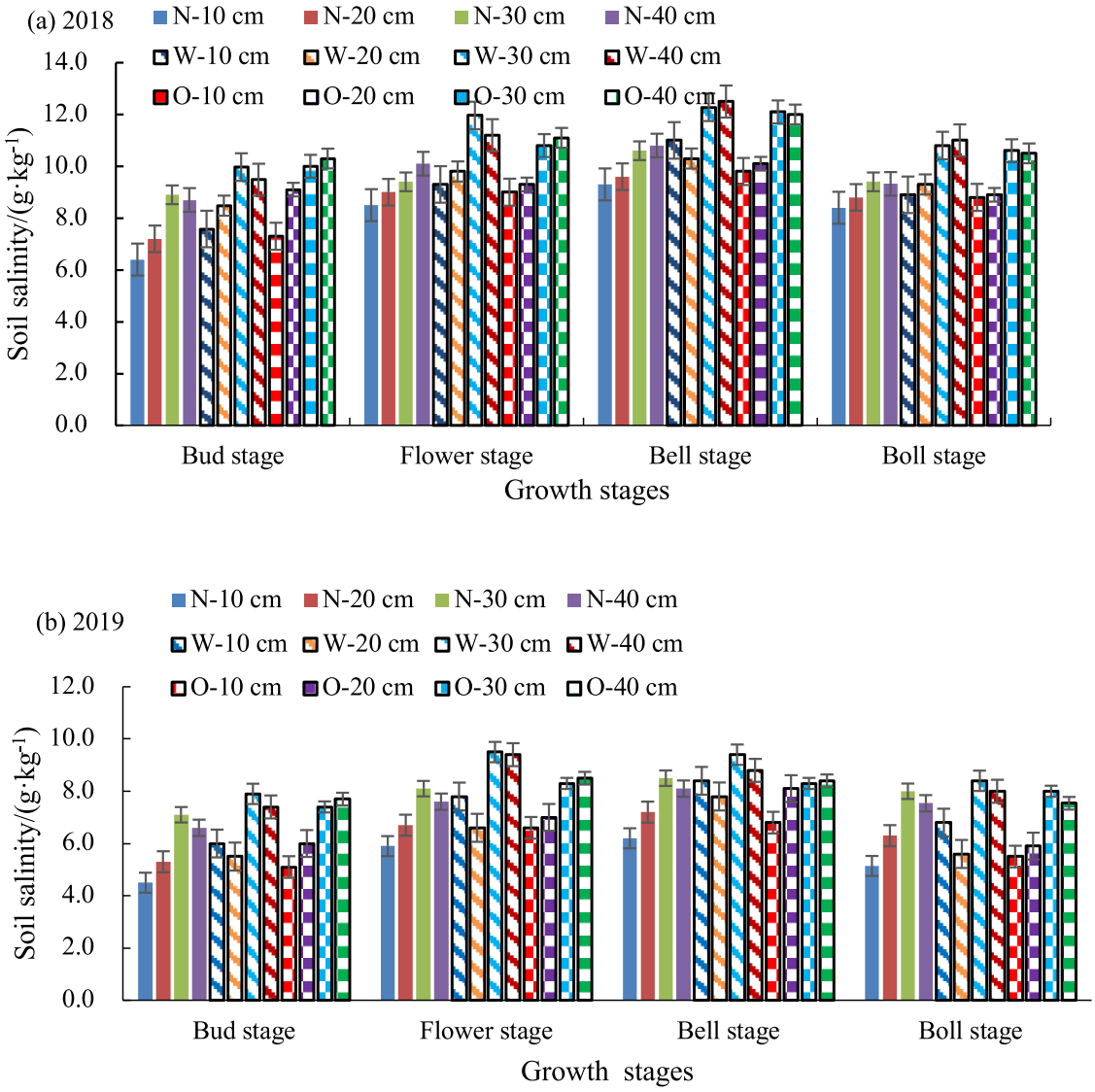

matrix (cm^2 min^{-1}), and q_i is a component of the fluid flux density.

2.4.3. Root uptake

The water stress response function model of Feddes et al. (1978) was used to account for water stress, and the threshold slope model of Khosla (1996) was used for salinity stress. Parameters of the water and salinity stress response functions were obtained from the literature (Feddes et al. 1978; Khosla 1996; Azad et al. 2018; Rahneshan et al. 2018). A multiplicative model was used to account for the combined effects of water and salinity stress (Kumar et al. 2021).

Cotton roots were sampled at a regular network of sampling points and measured using DT-SCAN (Chen et al. 2020). HYDRUS does not allow a temporally variable root zone. Therefore, a constant root distribution was used during the simulations (Wang et al. 2012).

2.4.4. Initial and boundary conditions

Measured soil water contents and salinities were used as the initial conditions in the flow domain.

$$\theta(z, 0) = \theta_i(z) \qquad t = 0, Z \le z \le 0 \tag{8}$$

$$c(z, 0) = c_i(z) \qquad t = 0, Z \le z \le 0 \tag{9}$$

where θ_i is the initial volumetric water content at different soil depths (cm^3 cm^{-3}), and c_i is the initial solute concentration at different soil depths (g L^{-1}).

Fig. 6. Distribution of water content at different positions in the soil profile during the growth stages in 2018. (a) Below dripper; (b) overlap zone. [Color online.]

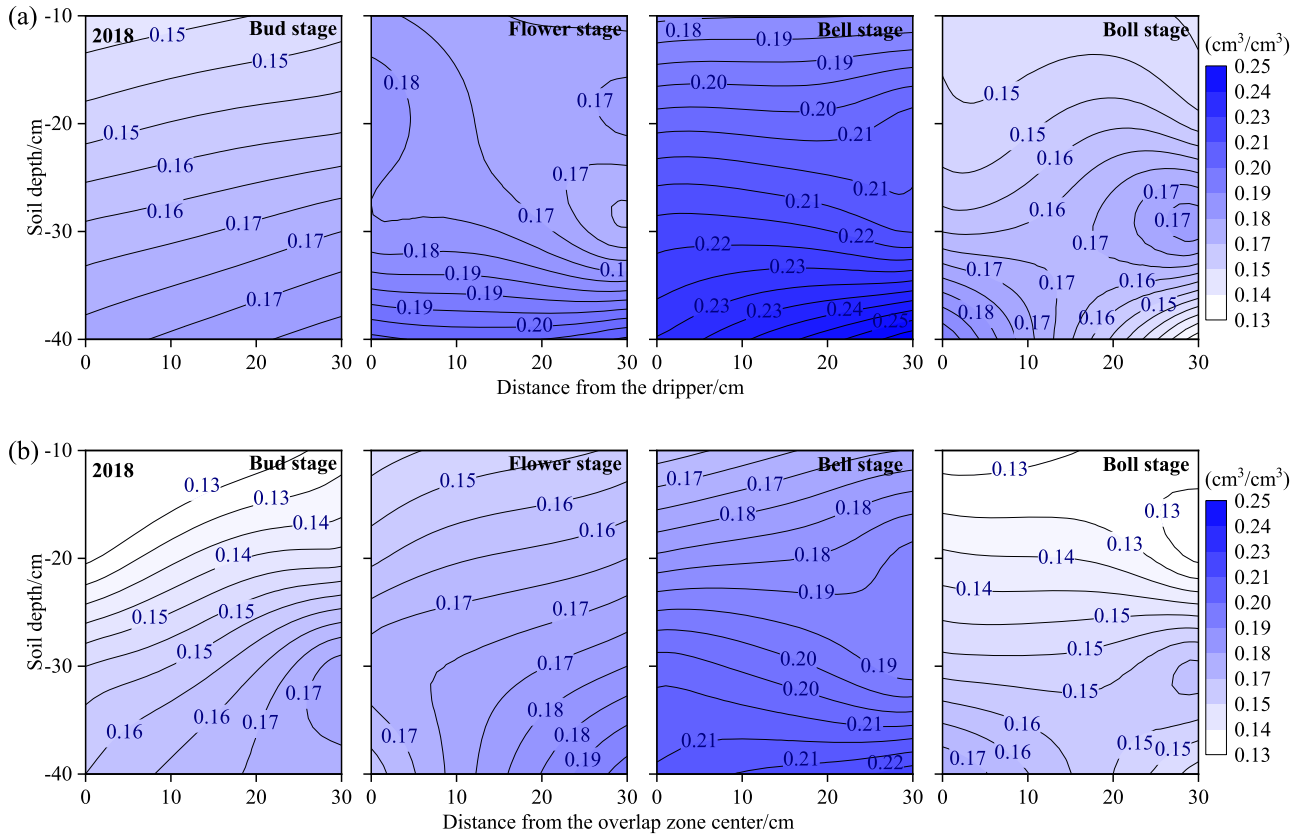

Temporally variable boundary conditions under the mulch were applied for evaporation and transpiration. Precipitation data were obtained from meteorological data. Daily precipitation and reference evapotranspiration (ET_o) were recorded by a weather station within 30 m of the experimental field. The daily crop potential evapotranspiration (ET_p) was calculated using the following equation:

$$ET_p = K_c \cdot ET_o \quad (10)$$

where K_c is the crop coefficient.

The ET_p consistsed of potential transpiration (T_p) and potential evaporation (E_p), which were described by the following equations (Campbell and Norman 1989):

$$T_p = \left(1 - e^{-k \cdot LAI}\right) ET_p \quad (11)$$

$$E_p = ET_p - T_p \quad (12)$$

where k is the radiation-extinction coefficient (0.58 for cotton; Srinet et al. 2019) and LAI is the leaf area index. LAI was measured as the one-sided green leaf area per unit ground surface; the green leaf area for each leaf was calculated as length × width × 0.703.

The variable-flux boundary condition for irrigation was based on the length of daily irrigation. Water volumes coupled with irrigation timing were used to determine the input values for the variable-flux boundary condition used as the drip irrigation source in the HYDRUS-3D simulation. An atmospheric boundary condition was used for bare soil. A constant-flux boundary condition was used along boundary elements representing emitters during the application of water in simulations of the field experiment. The constant boundary fluxes represented the corresponding measured fluxes of the field experiments. The flux was calculated by dividing the discharge rate by the ponded surface area of the boundary that represented an emitter in the HYDRUS model, because the HYDRUS model could not describe the changes in the ponded surface area. Thus, a constant value was chosen that was measured and calculated using the Bresler (1978) equation for 2018 and 2019. The emitter boundary became a zero-flux boundary after each irrigation. Zero-flux boundary conditions were also used for all three dimensions both during and after irrigation. A zero-flux condition was also used along the soil surface, because evaporation could be neglected due to the use of plastic mulch during irrigation. A free-drainage boundary condition was applied along the lower boundary. Running the HYDRUS-3D model required specifying the hydraulic parameters θ_r, θ_s, K_s, α, n, l, D_L (longitudinal dispersivity) and D_T (transverse dispersivity) (Table 2).

Fig. 7. Distribution of water content at different positions in the soil profile during the growth stages in 2019. (a) Below dripper; (b) overlap zone. [Color online.]

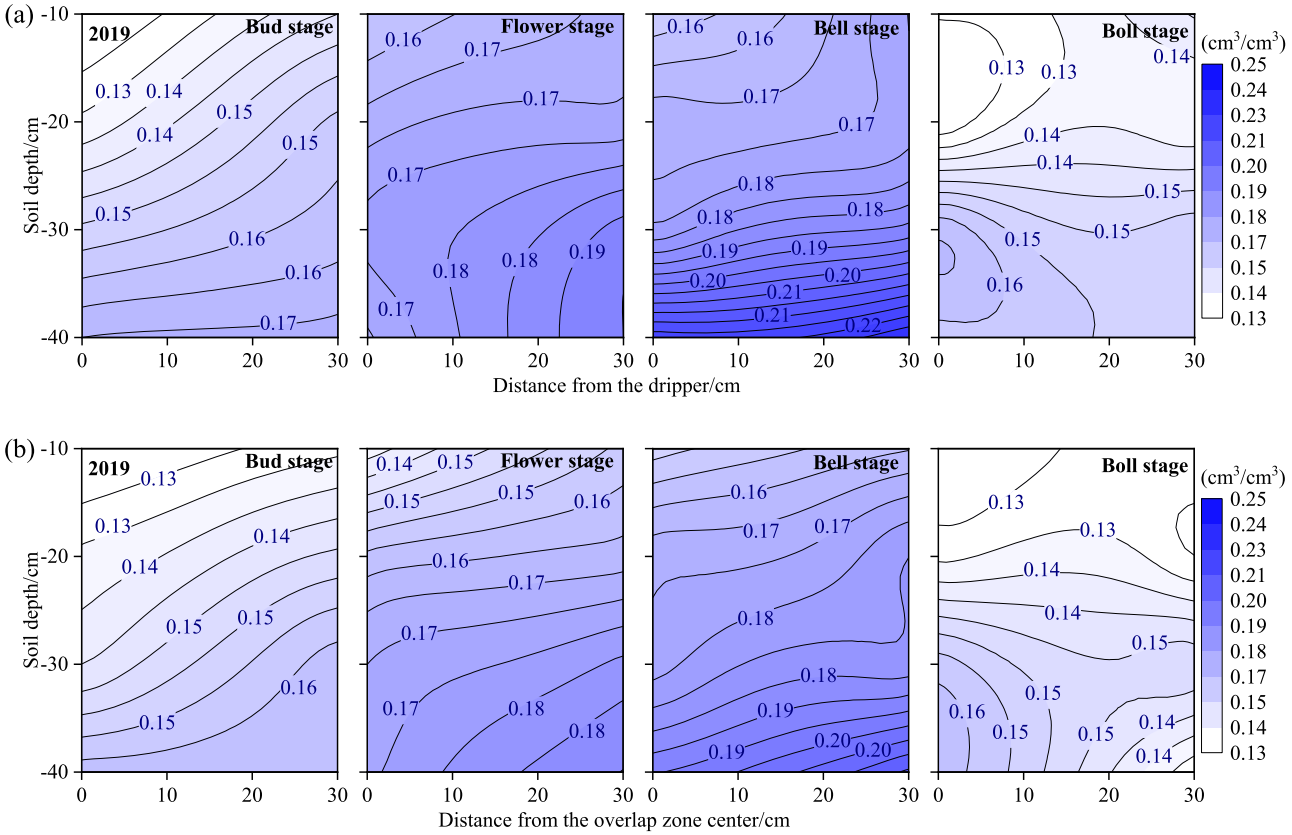

2.5. Statistical analysis

The performance of the model simulation was evaluated using three statistical indices. The coefficient of determination (R^2), mean absolute error (MAE), and the root mean square error (RMSE) quantified the differences between the observations and simulations, and were calculated using eqs. 13, 14 , and 15, respectively.

$$R^2 = \frac{\left[\sum_{i=1}^{N}\left(P_i-\bar{P}\right)\left(O-\bar{O}\right)\right]^2}{\sum_{i=1}^{N}\left(P_i-\bar{P}\right)^2\sum_{i=1}^{N}\left(O-\bar{O}\right)^2} \quad (13)$$

$$\mathrm{MAE} = \frac{1}{N}\sum_{i=1}^{N}|P_i - Q_i| \quad (14)$$

$$\mathrm{RMSE} = \sqrt{\frac{1}{N}\sum_{i=1}^{N}(P_i - Q_i)^2} \quad (15)$$

where P_i is a simulated value, O_i is an observed value, and N is the total number of observed values. $\bar{P}$ and $\bar{O}$ are mean of observed values and mean of simulated values, respectively.

3. Results and discussions

3.1. Model calibration and validation

Both model calibration and validation are prerequisites for effective model application. The water content and salinity data from the cotton seedling period were used to calibrate model parameters so as to ensure the reliability of the model used in this study. The water content and salinity data collected after the 12th irrigation in the bolling period were used as validation data. Figures 2 and 3 show the comparison of measured water and salinity and simulated values after the irrigation period of cotton seedlings (no irrigation) and the 12th irrigation in the bolling-open period, respectively.

We chose three indices for evaluating the accuracy of model simulations between the measured and simulated water content and salinity values: (*i*) the determination coefficient R^2 , which ranged from 0.89 to 0.97, (*ii*) the RMSE value, which ranged from 0.019 to 0.02 $cm^3\ cm^{-3}$ for soil water content and from 1.29 to 1.41 $g\ kg^{-1}$ for salinity, (*iii*) and the MAE value which ranged from 0.014 to 0.016 $cm^3\ cm^{-3}$ for soil water content and from 1.03 to 1.06 $g\ kg^{-1}$ for salinity. The reasons for model inaccuracy included the following: (*i*) the model assumed soil homogeneity, (*ii*) the measured root distribution and the actual distribution differed in detail, and (*iii*) the calculation of T_p and E_p had errors. LAI determined the accuracy of T_p. The relationship between T_p and LAI was positive but that between T_p and E_p was negative. Hence, T_p

Fig. 8. Distribution of salinity content at different positions in the soil profile during the growth stages in 2018. [Color online.]

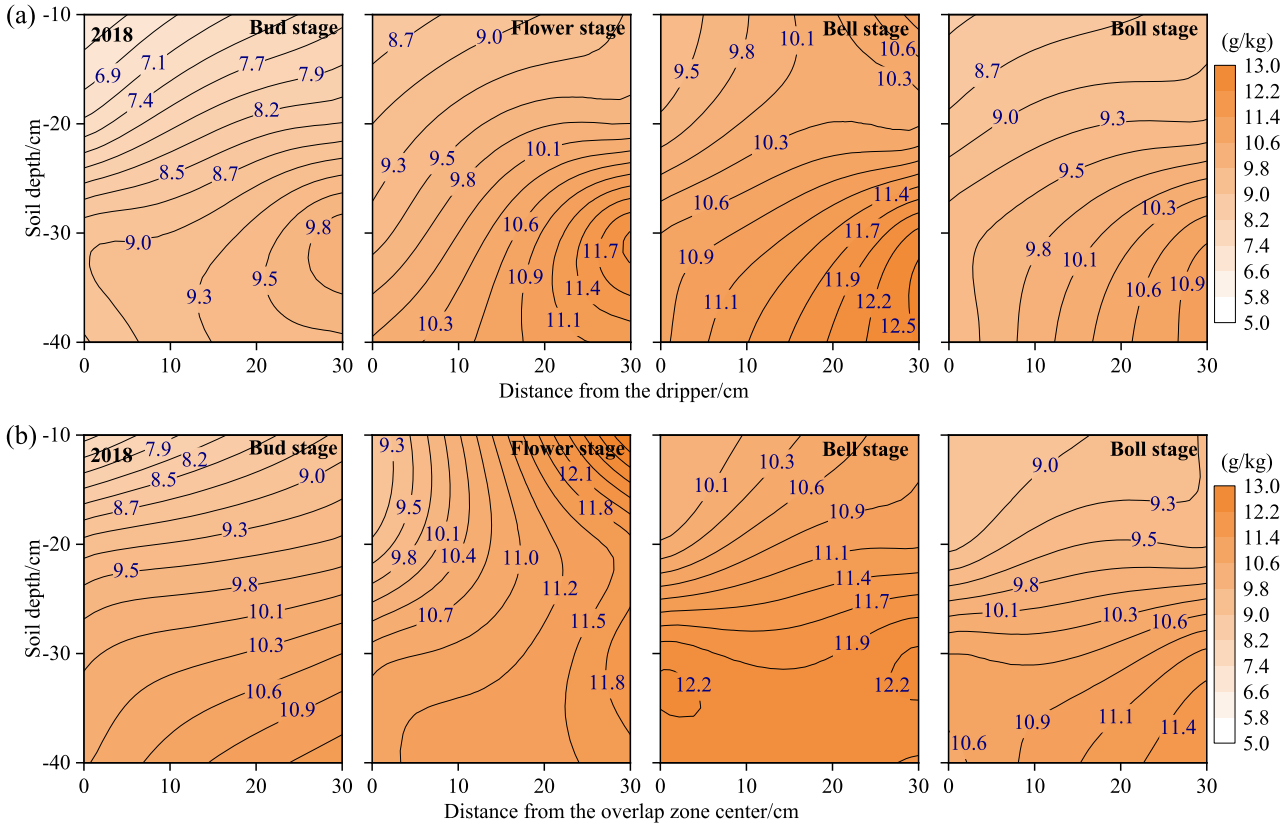

was overestimated if LAI was overestimated and E_p was underestimated, and the simulation might lead to water stress in the soil. T_p was underestimated if LAI was underestimated and E_p was overestimated, and the simulation might lead to salinity stress in the soil. Therefore, LAI should be measured carefully and frequently in various growth stages using accurate equipment. However, overall the results of the simulation presented in this study met the accuracy requirements, based on the results of Santhi et al. (2001). Therefore, the verified soil parameters (Table 2) could be used to simulate, predict, and design optimal irrigation systems.

3.2. Water content and salinity distributions and dynamics

The distribution and dynamic changes of water content and salinity are also important criteria for evaluating the accuracy of irrigation volume. Figures 4 and 5 show the water content and salinity changes at different locations in the 0–40 cm depth layers in four growth stages during 2018 and 2019. The analysis from the two perspectives of time and space suggested the following: (*i*) Time: Soil water content and salinity showed fluctuations, determined by cotton plant water consumption, imposed irrigation regime and water and salinity movement relationships. Throughout the growth period, the soil water content gradually decreased and the salinity content increased. The explanation was related to crop water consumption and soil evaporation, as well as salt being carried with irrigation water and returned to the soil by evaporation. (*ii*) Space: The water content of the upper soil was significantly lower than that of the lower layer, while the salinity increased with depth. The water content of the narrow stripe was higher than wide stripe, while the salinity was compared with that of the wide stripe. The reasons might be as follows: (*i*) Cotton roots with drip irrigation were mainly distributed in the 0–30 cm depth layer and thus consumed water in this layer. (*ii*) Evaporation and crop water absorption transported water from deep to shallow layers, water was absorbed by the crop, and salt was left in the soil. (*iii*) The drip line was laid in the narrow stripes, where leaching of salt into deep soil occurred, moving it away from the drip line.

The aforementioned conclusions were consistent with the findings of Li et al. (2018). In addition, the overlap zone water content and the salinity distributions were found to be basically the same below the drippers, but the water content was lower than that below the drippers, while the salinity distribution was the opposite. The reasons for this were as follows: (*i*) soil below the drippers was exposed to more irrigation than the soil in the overlap zone. (*ii*) The root water consumption in the overlap zone was greater than that below the dripper and led to greater salt accumulation in the overlap zone. In addition, the analysis of both years suggested that the soil water content was in the following order: bell stage > flower stage > bud stage > boll stage. The soil salt accumulation also increased from the bud to the flower stage over the 2 years, which was 16% and 20%, respectively. The largest drop in salinity occurred from the bell to the bolling period over the 2 years, by 16% and 9%, respectively. The change in salinity

Fig. 9. Distribution of salinity content at different positions in the soil profile during the growth stages in 2019. (a) Below dripper; (b) overlap zone. [Color online.]

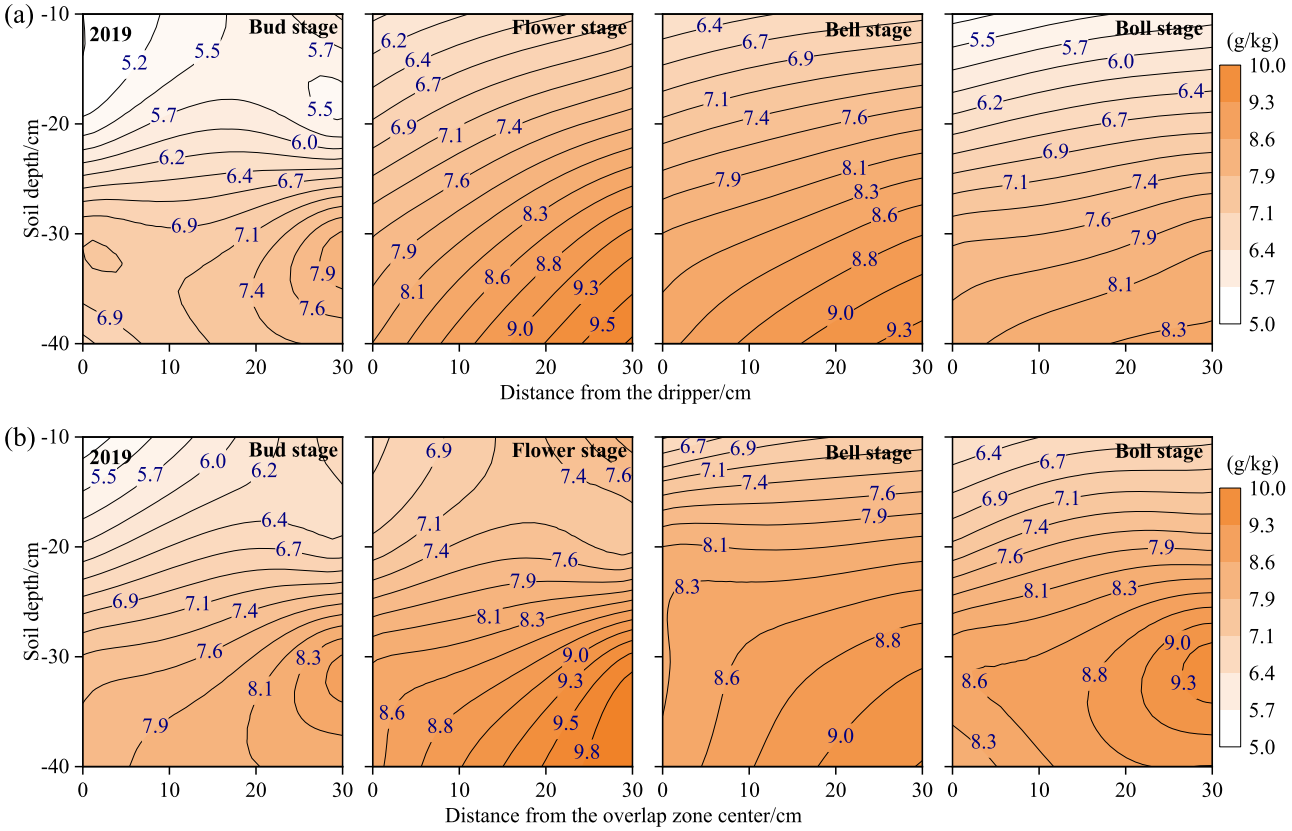

Table 3. Scheme of simulations.

Case	Emitter discharge (L h^{-1})	Emitter spacing (cm)	Initial water content (cm^3 cm^{-3})	Irrigation volume (L)	Salinity content (g kg^{-1})
I	1.8, 2.4, 3.2	30	0.15		
II	1.8	20, 30, 40	0.15	10	5
III	1.8	30	0.15, 0.175, 0.2		

from the flower to the bell stage was not significant, being 5% and −1.5%, respectively. These results reflected the effect of water movement and salt transport on cotton water demand and the irrigation regime.

3.3. Evaluation of an optimal irrigation volume

An optimal water irrigation rate should ensure that water and nutrients are evenly distributed in the soil to meet the needs of crop growth. The salinity tolerance threshold of cotton and the water–salinity distributions in the drip irrigation overlap zone were fully considered in this study, and a suitable irrigation volume was determined using the HYDRUS-3D model (shown in Table 1). Figures 6–9 show the observed water content and salinity distributions of contours in the 0–40 cm depth range at different positions for the years 2018 and 2019. As can be seen from the figures, the water content displayed a trend of increasing first and then decreasing, while the salinity increased first and then decreased. The reasons were as follows: (*i*) with the increase of cotton water demand, the water demand in the later fertility period of cotton growth increased. (*ii*) As irrigation increased, salt transport increased, and water absorption by the cotton also drew salt from lower soil layers to upper layers. The soil salinity had a tendency to decline with decreasing soil water demand and evaporation strength. The average water content of the soil root layer below drippers was 0.161, 0.174, 0.206, and 0.157 cm^3 cm^{-3} in 2018 and 0.15, 0.173, 0.187, and 0.144 cm^3 cm^{-3} in 2019; the overlap zone was 0.146, 0.166, 0.191, and 0.144 cm^3 cm^{-3} in 2018 and 0.145, 0.17, 0.178, and 0.140 cm^3 cm^{-3} in 2019 in the bud, flower, bell, and boll stages, respectively. The soil water content at the below drippers was 66%, 75%, 84%, and 65% in 2018 and 62%, 71%, 77%, and 59% in 2019 of the water-holding capacity in the field; the overlap zone was 60%, 68%, 78%, and 59% in 2018 and 60%, 71%, 73%, and 58% in 2019 in the bud, flower, bell, and boll stages, respectively. The salinity average values of soil root layer at different positions were as follows: below dripper: 8.34, 9.91, 10.8, and 9.49 g kg^{-1} in 2018 and 6.3, 7.7, 7.69,

Fig. 10. Distribution of water content at different positions with various dripper discharge rates in the profile. (a) Below dripper; (b) overlap zone. [Color online.]

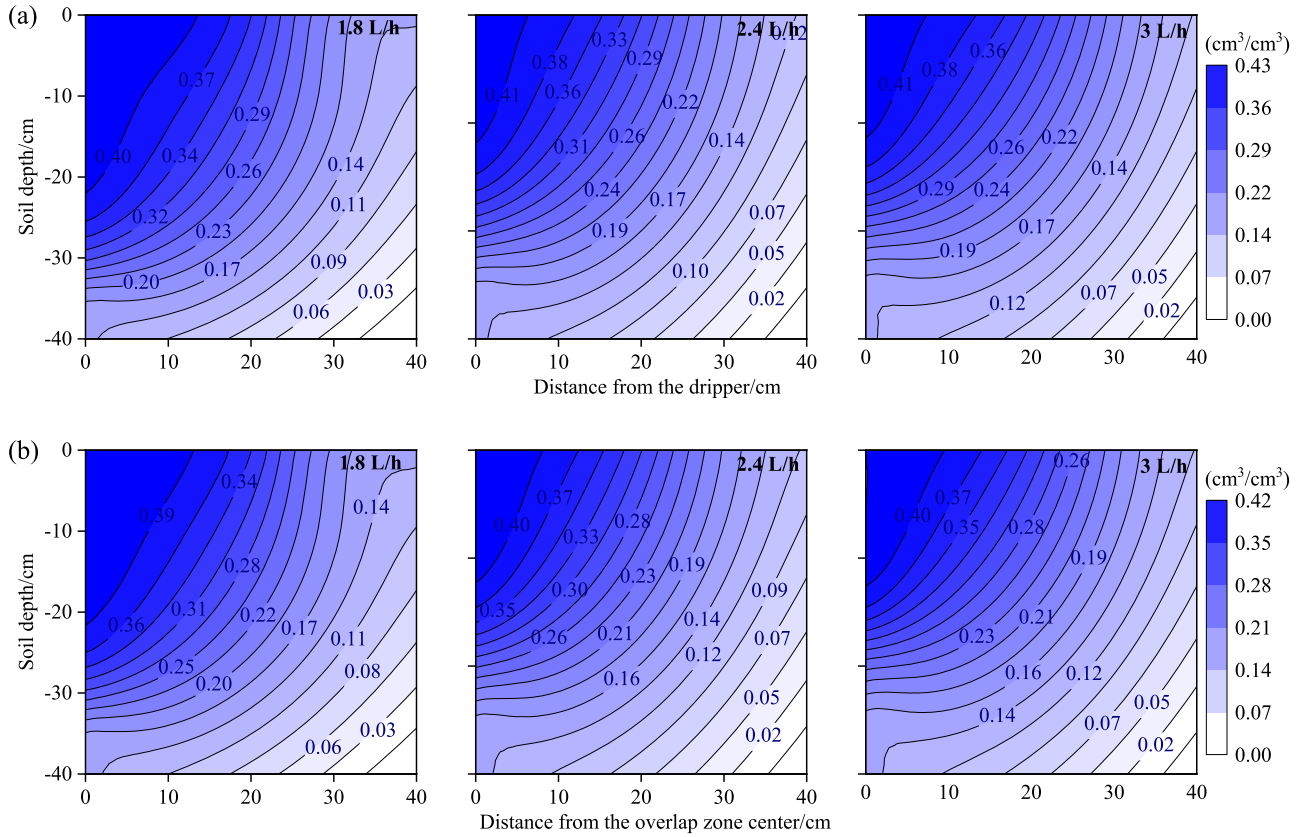

and 6.97 g kg^{-1} in 2019; the overlap zone was 9.63, 11.14, 11.26, and 9.3 g kg^{-1}in 2018 and 7, 8.16, 7.91, and 7.17 g kg^{-1} in 2019 in the bud, flower, bell, and boll stages in 2018 and 2019, respectively. The comparison of the cotton water–salinity thresholds in different periods given by Meng et al. (2008) and Chen (2010) showed that the soil water content met the cotton water stress threshold in 2018 and 2019, while the soil salinity in the bud, flower, and bell stages exceeded the salinity tolerance threshold in 2018. The comparison of results revealed that the irrigation watering scheme applied in the bud and bell stages in 2018 was not enough, while the irrigation watering scheme designed using the model in 2019 ensured that no water stress and salinity stress occurred in the cotton reproductive stage. This confirmed that the developed irrigation water volume was optimal. It also proved that the HYDRUS-3D model could be used as an effective tool to formulate irrigation regimes. Possible reasons for the difference between the irrigation watering scheme designed by Wang et al. (2012) and the current scheme were as follows: (*i*) consideration of the water and salinity stress thresholds in the different growth stages of cotton, (*ii*) consideration of the three-dimensional movement of drip irrigation water and the water–salinity environment of the soil with drip irrigation in the overlap zone, and (*iii*) groundwater burial depth below 5 m that resulted in no water supply to the crop.

3.4. Evaluation of technical parameters

Consideration must be given to the soil type, initial conditions, drip irrigation technical parameters, crops, and other factors to design an optimal drip irrigation watering scheme. The initial water content, emitter discharge, and emitter spacing were selected for simulation. The specific scheme used in this study is shown in Table 3. Uniformity (CU) and leaching rate (L_r) were used in the model evaluation to analyze the impact and recommend optimal design parameters. The following equations were used:

$$\text{CU} = \left[1 - \frac{\sum_{i=1}^{N} |P_i - \bar{P}|}{\sum_{i=1}^{N} P_i}\right] \times 100 \quad (16)$$

$$L_r = \frac{S_i - S_f}{S_i} \times 100 \quad (17)$$

where P_i is a simulated value, $\bar{P}$ is the mean of simulated values, and N is the total number of simulated values. S_i and S_f are initial soil salinity and final soil salinity, respectively.

Fig. 11. Distribution of salinity content at different positions with various dripper discharge rates in the profile. (a) Below dripper; (b) overlap zone. [Color online.]

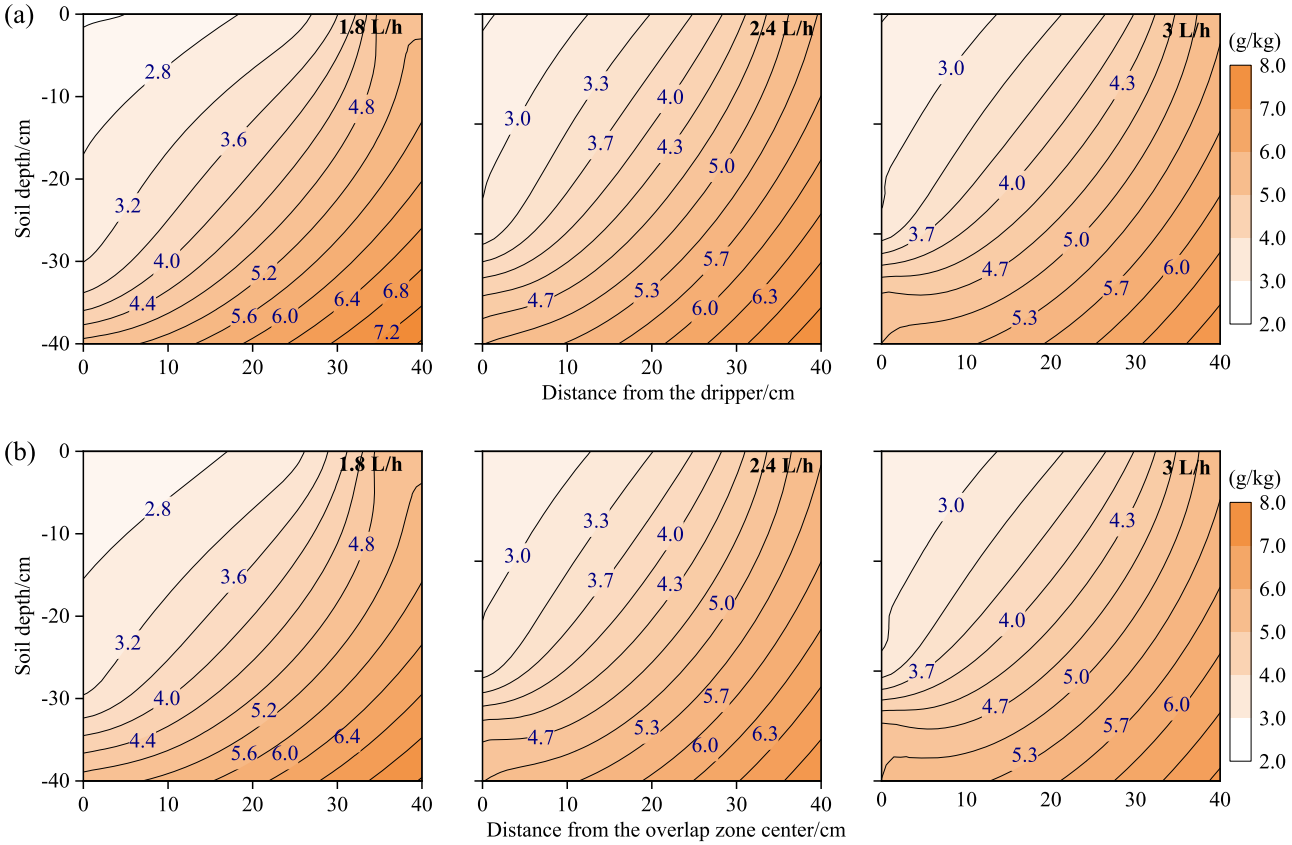

Table 4. Leaching rates with different emitter discharge rates.

Positons	Depth (cm)	Emitter discharge (L h^{-1})			Relationship between leaching and emitter discharge
		1.8	2.4	3	
Below dripper	10	48.9	48.4	47.8	
	20	44.2	43.9	43.5	
	30	39.1	38.5	38.3	L_r=−0.0158E_d + 0.3795
	40	12.6	7.9	3.8	(R^2 = 0.993)
Overlap zone	10	47.1	47.3	47.6	L_r: Leaching rate
	20	43.1	43.4	43.6	E_d: Emitter discharge
	30	37.5	38	38.5	
	40	9.2	5.5	2.6	

3.4.1. Emitter discharge

Surface ponding is a common phenomenon in farmlands during the irrigation process (REF). For drip irrigation, the emitter discharge rate determines the range of water conditions on the soil surface, thus affecting the speed of the wetting front and the confluence time of the wetting front, consequently, the spatial range of the wetted body and the distribution of water and salinity. Therefore, understanding the water–salinity distribution under the confluence of different emitter discharges is necessary to provide a basis for choosing a reasonable emitter discharge rate. Figure 10 shows the contour diagrams of the distribution of soil water content at different positions under emitter discharge rates of 1.8, 2.4, and 3 L h^{-1}. Under the three discharge rates treatments, the water content decreased with increasing distance from the dripper and the overlap zone center. However, a comparison between treatments at the same position suggested that the water content increased with an increase in emitter discharge in the horizontal direction of the dripper and overlap zone, while it showed an opposite change pattern in the vertical direction. The reason for this phenomenon was that when the emitter discharge was larger, the surface ponding was larger. The water movement was faster in the horizontal direction over a larger distance, while it was smaller in the vertical direction.

Fig. 12. Distribution of water content at different positions with various dripper spacing in the profile. (a) Below dripper; (b) overlap zone. [Color online.]

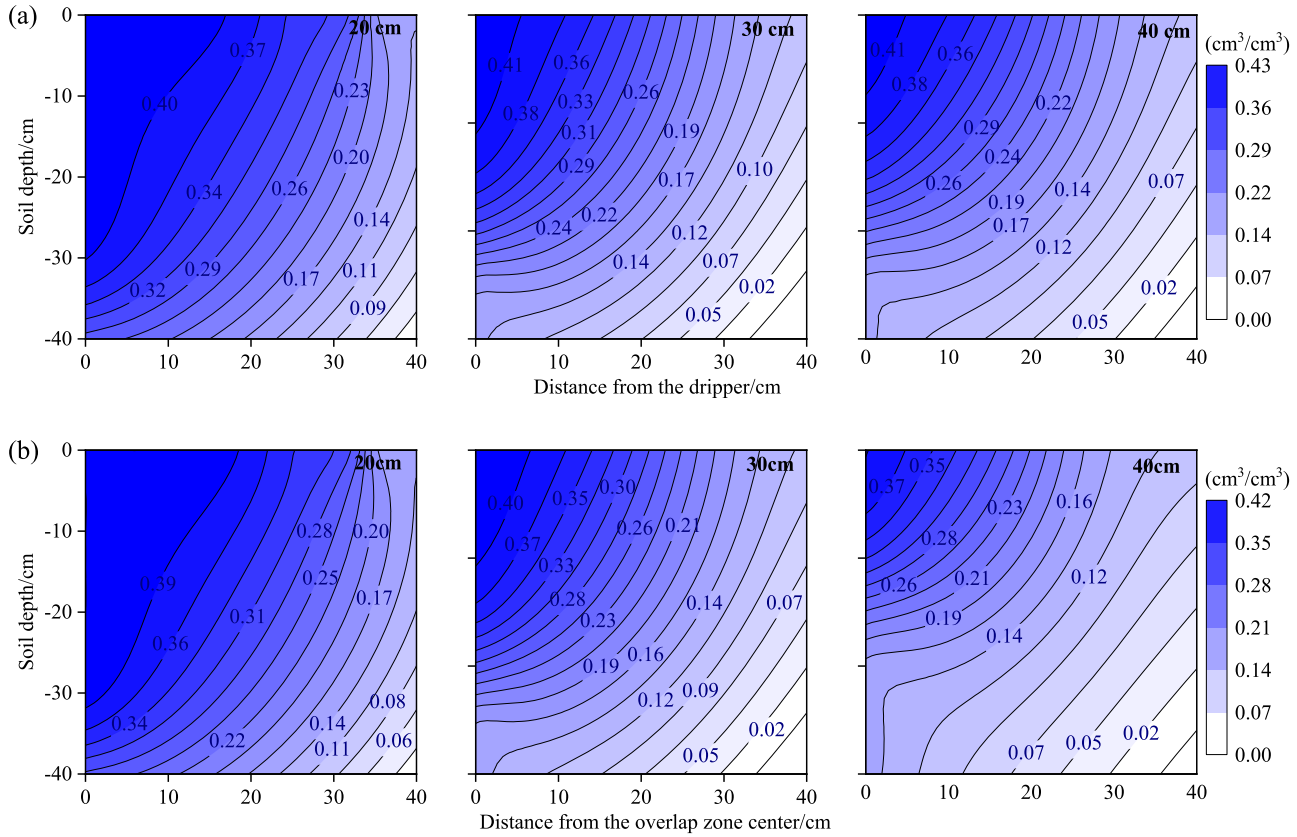

Figure 11 shows the salinity distribution diagram with various emitter discharge rates at different positions. The treated salinity increased with distance from the dripper and the center of the overlap zone, indicating the movement relationship of "salt moves with water flow". The salinity at the same position below the dripper and in the overlap zone between the treatments decreased with an increase in emitter discharge rate in the horizontal, while the vertical direction showed the opposite relationship. The reason was that when the emitter discharge was greater, more water there moved in the horizontal direction, which promoted salinity leaching. The vertical water flow reduced, leading to the wash of salinity. When the emitter discharge rate was smaller, the effect was the opposite. These results indicated that a greater emitter discharge rate promoted water–salinity movement in the horizontal direction, while a lower emitter discharge rate promoted water–salinity movement in the vertical direction. This conclusion was consistent with the fingings of Goldberg et al. (1971), Li et al. (2012), and Huang et al. (2019).

Uniformity is an important indicator in evaluating irrigation quality. Statistical calculations found that each treatment uniformity decreased with increasing emitter discharge rate, and a linear relationship between the two could be expressed as ($CU = -0.0092E_d + 0.9177$, $R^2 = 0.992$). The results of the present study were consistent with the findings of El-hafedha et al. (2001). However, Li et al. (2007) found that the uniformity increased with an increase in the emitter discharge; the discrepancies in results might be due to different soil textures or irrigation methods. In addition, the leaching rate was also an important indicator reflecting the irrigation quality. The statistical results on leaching rates for different emitter discharge rates are shown in Table 4. The leaching rates at different locations decreased with increasing soil depth. The leaching rate at 0–30 cm depth decreased with the emitter discharge rate, while the overlap zone showed the opposite trend. This was probably because greater emitter discharge rate resulted in higher water content in the upper soil in the overlap zone compared with the smaller emitter discharge rate. Furthermore, the analysis of the wet body leaching rate revealed that it decreased with increasing emitter discharge rate. A linear relationship between the two is shown in Table 4. The results indicated that larger emitter discharge rates should be chosen for crops with large planting spacing in actual production, and smaller emitter discharge rates for crops with deeper roots.

3.4.2. Emitter spacing

The emitter spacing determines not only the number of drippers, but also the time when the wet front meets, thus affecting the wet front advance speed, wet body range, and water–salinity distribution. Figure 12 shows contour diagrams of water distribution at different locations under three

Fig. 13. Distribution of salinity content at different positions with various dripper spacing in the profile. (a) Below dripper; (b) overlap zone. [Color online.]

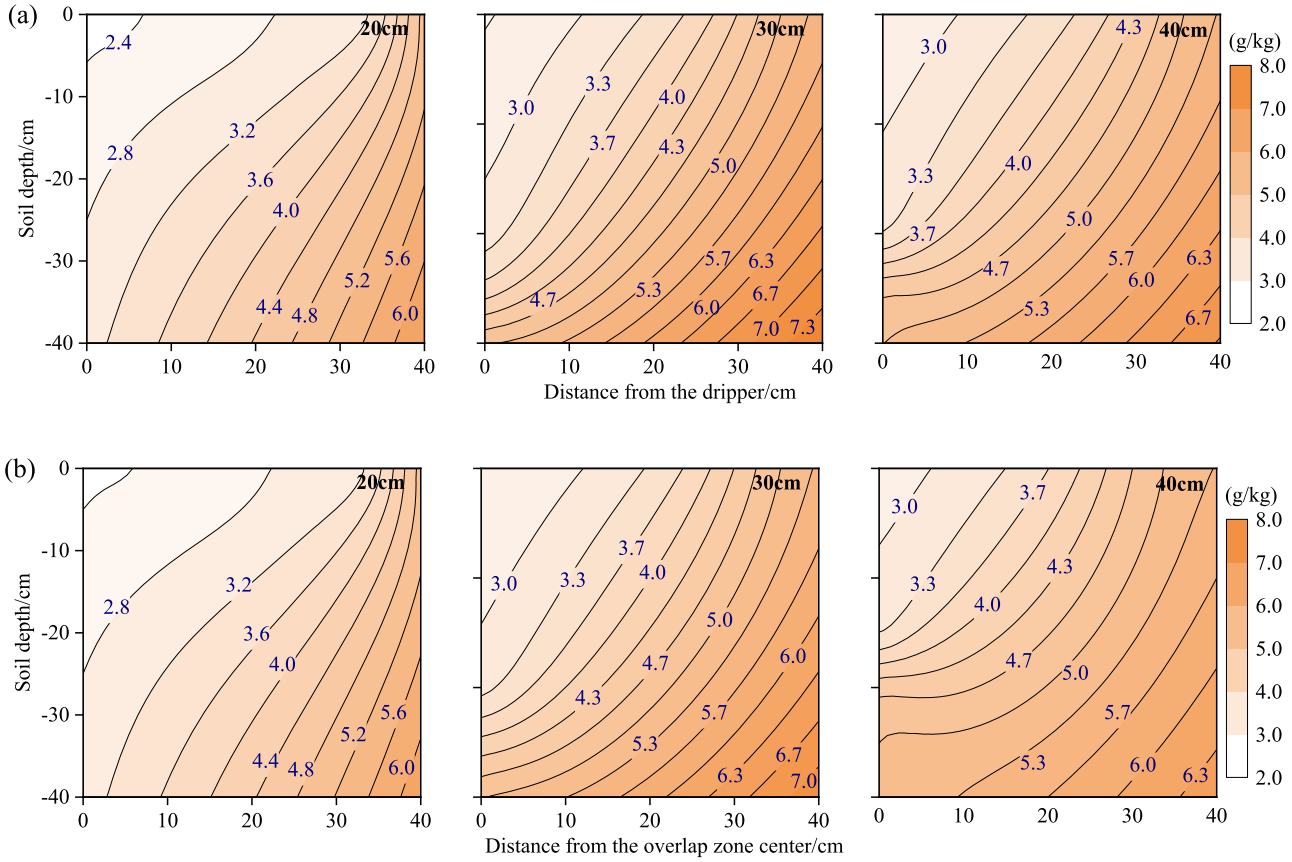

Table 5. Leaching rate with different emitter spacings.

	Depth (cm)	Emitter spacing (cm)			Relationship between leaching and emitter discharge
		20	30	40	
Below the emitter	10	51.2	48.9	46.7	
	20	47.2	44.2	41.7	
	30	44.3	39.1	35.3	$L_r = 2.5164d^{-0.575}$
	40	40.1	12.6	4.6	($R^2 = 0.993$)
Overlap zone	10	51	47.1	43.8	L_r: Leaching rate
	20	46.8	43.1	39.7	d: Emitter spacing
	30	43.2	37.5	21.5	
	40	39.8	9.2	1	

emitter spacing confluence conditions. The water distribution under all treatments decreased with increasing distance from the dripper and the overlap zone. The water content at the same position between the treatment decreased with increasing emitter spacing, probably because when the emitter spacing was small, the wetting front was met quickly and the speed of the wet front was faster, finally resulting in a large wet range.

The salinity content is analyzed in Fig. 13. The figure shows that the salinity content under all treatments tended to increase with distance from the dripper and the center of the overlap zone. The salinity at the same position between each treatment increased with increasing emitter spacing. This was probably because when the emitter spacing was small, the short confluence time accelerated water promotion, promoting salinity leaching. Also, the confluence time was long under large emitter spacing conditions, and the water movement was slow.

According to the irrigation uniformity of the three emitter calculations, it was found that uniformity decreased when the emitter spacing increased, and that the relationship could be expressed in a power function relationship ($CU = 1.1815d^{-0.08}$, $R^2 = 0.992$). The reason was as follows: when the emitter spacing was small, the confluence time was

Fig. 14. Distribution of water content at different positions with various initial water content in the profile. (a) Below dripper; (b) overlap zone. [Color online.]

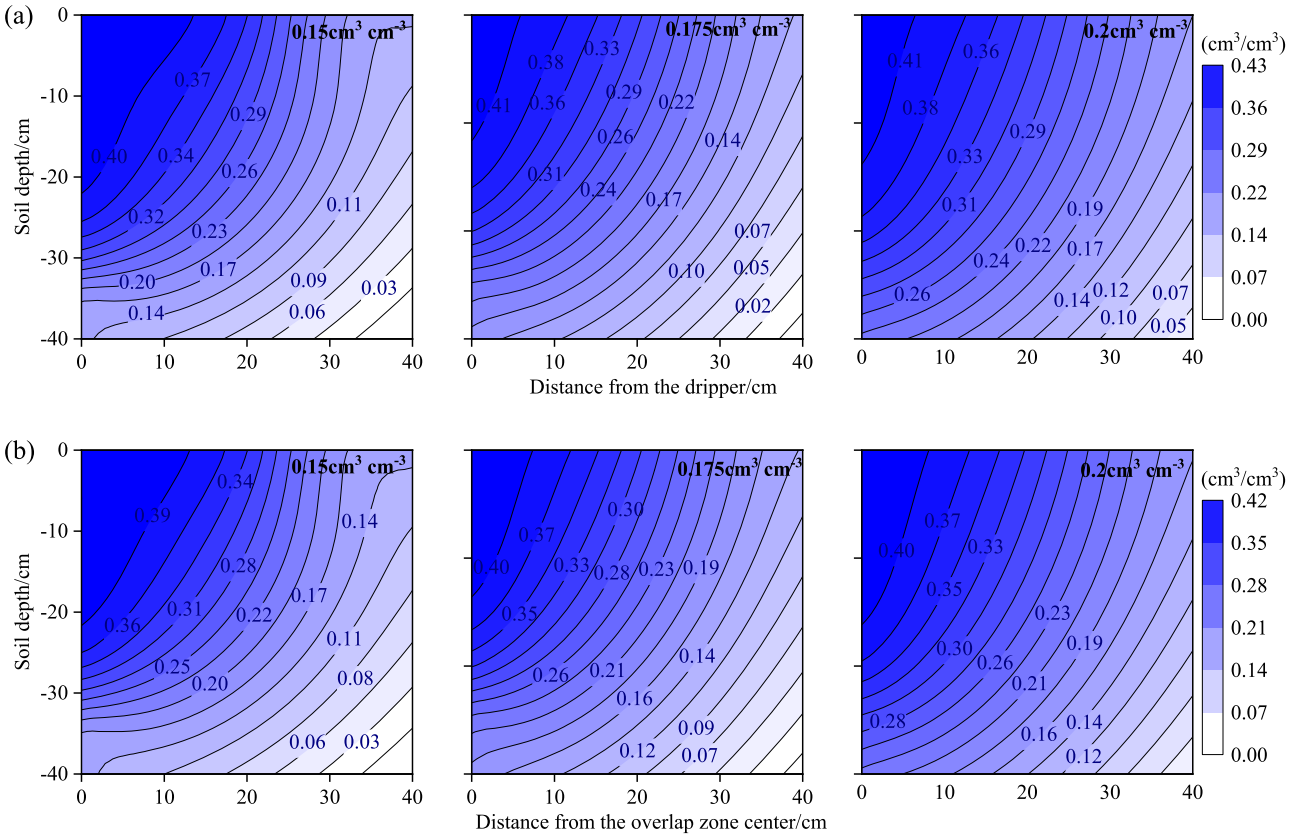

short. The soil water propulsion led to a rapid increase in the soil water content, the shorter the time of saturation, the larger the soil saturation range. The analysis of the leaching rate with different emitter spacings is shown in Table 5. The leaching rates under all treatments decreased with increasing depth and increased with increasing emitter spacing. The inter-treatment analyses found a negative correlation between leaching rate and emitter spacing and a power function relationship between the two could be expressed, as shown in Table 5. The results indicated that a smaller emitter spacing was not only conducive to improving the uniformity of irrigation, but also promoted the leaching rate of soil salinity, which was recommended for use in high dense planting farmland.

3.4.3. Initial soil water content

Soil initial moisture content is an important basis for calculating reasonable irrigation volumes. Figure 14 shows the water distribution with three initial water content treatments under confluence conditions. The water content distribution relationship was consistent with the analysis results of the aforementioned two factors. Between different treatments, the wetted body was proportional to the initial water content. The water content increased with the increase in the initial moisture content at the same positions; the greater the initial water content, the shorter the time for saturation. Hence, at the same time, the water advanced faster and with a greater wetted range. The results of this study were consistent with the findings of Niu et al. (2012) and Ma et al. (2020). However, they were inconsistent with the results of Zeng et al. (2010) and Chen et al. (2006). The reasons for this were as follows: (*i*) various soil textures and (*ii*) different ways of water infiltration and different boundary conditions formed by different irrigation methods. Figure 15 shows the salinity distributions under all treatments, where the salinity distribution trend was consistent with the results of the first two factors. A comparative analysis between different treatments found that the range of leaching rate was proportional to the initial water content, and the salinity at the same position also decreased with increasing the initial water content. The reason was that the initial water content had a promoting effect on water movement, thus accelerating the leaching of soil salinity. However, Yin et al. (2011) found a negative correlation between the initial water content and the leaching rate. The inconsistent results might be due to different soil textures and water–salinity contents in the soil.

The statistical analysis of the irrigation uniformity of different initial water content rates showed (such as in Table 6) that the irrigation uniformity increased with increasing initial water content due to the following reasons: (*i*) large initial water content, small water potential gradient change, and gentle water movement; and (*ii*) large initial water content and short arrival saturation time promoting the move-

Fig. 15. Distribution of water content at different positions with various initial water content in the profile. (a) Below dripper; (b) overlap zone. [Color online.]

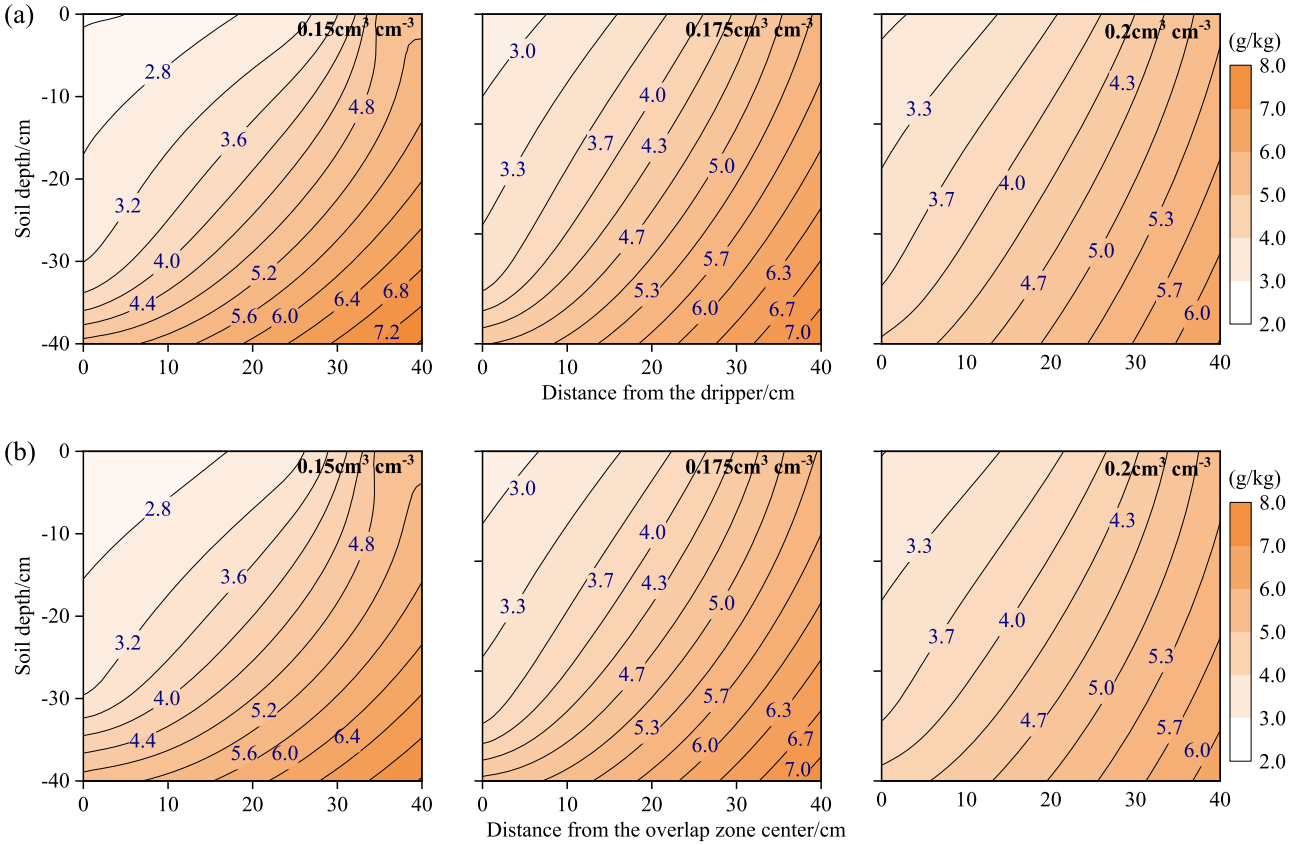

Table 6. Leaching rate with different initial water content rates.

Positions	Depth (cm)	Initial water content (cm^3 cm^{-3})			Relationship between leaching and initial water content
		20	30	40	
Below dripper	10	48.9	45.5	42.9	
	20	44.2	40	37	
	30	39.1	34.3	31.4	$L_r = 0.238\theta_{in}^{-0.204}$
	40	12.6	17.3	22.7	($R^2 = 0.996$)
Overlap zone	10	47.1	44	41.3	L_r: Leaching rate
	20	43.1	39.5	36.5	θ_{in}: Initial water content
	30	37.5	34	31.3	
	40	9.2	15.5	21.8	

ment of water. The analysis revealed that a linear relationship between the two could be described by (CU = 0.5852 θ_{in} + 0.8109, R^2 = 0.995). Niu et al. (2012) examined the effect of varying initial water content treatments on soil infiltration with bubble irrigation and found that the soil wetted body and uniformity increased with increasing initial water content. They suggested that the soil water movement velocity was not completely determined by the value of the soil matrix potential. During irrigation, soil pores needed to be filled. When the initial water content was smaller, more water needed to be filled. Also, the saturation state was longer and the wetting front movement was slower.

4. Conclusions

Suitable and safe use of brackish water is an important development needed to resolve fresh water scarcity, avoid soil secondary salinization, and ensure crop health development in arid and semi-arid regions. In this study, the HYDRUS model was used as an effective tool for designing a suitable irrigation volume based on cotton water stress thresholds and salinity thresholds in various growth stages. Technical parameters, such as emitter discharge rate, emitter spacing, and initial water content were chosen, simulated, and analyzed. The conclusions were as follows: the emitter discharge rate and emitter spacing were negatively associated with the ir-

rigation uniformity and desalination rate. The initial water content and irrigation uniformity and desalination rate correlated positively. The technical parameters with small emitter discharge and small emitter spacing should be selected in a drip irrigation system for improving irrigation uniformity and desalination rate. In addition, some other factors need further study, such as soil texture, soil temperature, depth of ground water table, and so on. Future versions of the model must incorporate root development to minimize simulation error, besides using advanced equipment to measure the parameters carefully in various growth stages.

Acknowledgements

We thank the editor and anonymous reviewers for comments that greatly improved the manuscript.

Article information

History dates

Received: 22 March 2022
Accepted: 23 May 2022
Accepted manuscript online: 17 June 2022
Version of record online: 14 November 2022

Copyright

Data availability

Data generated or analyzed during this study are provided in full within the published article.

Author information

Author ORCIDs

Su Lijun https://orcid.org/0000-0002-2271-9038

Author contributions

Yuyang Shan: Software, Writing – original draft. Lijun Su: Methodology, Supervision. Quanjiu Wang: Supervision. Yan Sun: Formal analysis, Writing – review & editing. Weiyi Mu: Data curation. Jihong Zhang: Writing – review & editing. Kai Wei: Data curation.

Competing interests

The authors declared that they have no conffiicts of interest in this work.

Funding information

This work was financed by the National Natural Science Foundation of China (51979220, 41907010), the Major Science and Technology Projects of the XPCC (2021AA003-2) and Special Scientific Research Project of Education Department of Shaanxi Province (21JK0783).

References

Ali, R., and Elliott, R.L. 2000. Soil salinity modeling over shallow water tables. I: validation of LEACHC. J. Irrig. Drain. Eng. **126**: 223–233. doi:10.1061/(ASCE)0733-9437(2000)126:4(223).

Azad, N., Behmanesh, J., Rezaverdinejad, V., Abbasi, F., and Navabian, M. 2018. Developing an optimization model in drip fertigation management to consider environmental issues and supply plant requirements. Agric. Water Manage. **208**: 344–356. doi:10.1016/j.ag w at. 2018.06.030.

Bresler, E. 1978. Analysis of trickle irrigation with application to design problems. Irrig. Sci. **1**: 3–17. doi:10.1007/BF00269003.

Bustan, A., Cohen, S., Malach, Y.D., Zimmermann, P., and Golan, R. 2005. Effect of timing and duration of brackish irrigation water on fruit yield and quality of late summer melon. Agric. Water Manage. **74**: 123–134. doi:10.1016/j.agwat.2004.11.009.

Bustana, A., Sagia, M., Malach, Y.D., and Pasternak, D. 2004. Effects of saline irrigation water and heat waves on potato production in an arid environment. Field Crops Res. **90**: 275–285. doi:10.1016/j.fcr. 2004.03.007.

Campbell, G.S., and Norman, J.M. 1989. The description and measurement of plant canopy structure. Society for experimental biology. Cambridge University Press, Cambridge. pp. 1–19. doi:10.1038/npre. 2011.5790.1.

Chamekh, Z., Ayadi, S., Karmous, C., Trifa, Y., Amara, H., Boudabbous, K., et al. 2016. Comparative effect of salinity on growth, grain yield, water use efficiency, δ13C and δ15N of landraces and improved durum wheat varieties. Plant Sci. **251**: 44–53. doi:10.1016/j.plantsci.2016.07. 005. PMID: 27593462.

Che., Z., Wang, J., and Li, J.S. 2021. Effects of water quality, irrigation amount and nitrogen applied on soil salinity and cotton production under mulched drip irrigation in arid northwest China. Agric. Water Manage. **247**: 106738. doi:10.1016/j.agwat.2021.106738.

Chen, H.S., Shao, M.A., and Wang, K.L. 2006. Effects of initial water content on hillslope rainfall infiltration and soil water redistribution. Trans. CSAE, **22**: 44–47. doi:10.3321/j.issn:1002-6819.2006.01.010.

Chen, M., Kang, Y.H., Wan, S.Q., and Liu, S.P. 2009. Drip irrigation with saline water for oleic sunflower (*Helianthus annuus* L.). Agric. Water Manage. **96**: 1766–1772. doi:10.1016/j.agwat.2009.07.007.

Chen, W.L., Jin, M.G., Ferréc, Ty.P.A., Liu, Y.F., Huang, J.O., and Xian, Y. 2020. Soil conditions affect cotton root distribution and cotton yield under mulched drip irrigation. Field Crops Res. **249**: 107743. doi:10. 1016/j.fcr.2020.107743.

Chen, X. L. 2010. Study on threshold value of irrigation with saline water and response function of cotton yield to salt with drip irrigation under mulch. Xin Jiang Institute of Ecology and Geography Chinese Academy of Sciences. doi: http://ir.xjlas.org/handle/365004/11142.

Chen, X., Qi, Z., Gui, D., Sima, M.W., Zeng, F. Li, L., et al. 2020. Evaluation of a new irrigation decision support system in improving cotton yield and water productivity in an arid climate. Agric. Water Manage. **234**: 106139. doi:10.1016/j.agwat.2020.106139.

Cucci, G., Lacolla, G., Boari, F., Mastro, M.A., and Cantore, V. 2019. Effect of water salinity and irrigation regime on maize (*Zea mays* L.) cultivated on clay loam soil and irrigated by furrow in southern Italy. Agric. Water Manage. **222**: 118–124. doi:10.1016/j.agw at.2019.05.033.

Del, Amor. F.M., Martinez, V., and Cerdá, A. 2001. Salt tolerance of tomato plants as affected by stage of plant development. HortScience, **36**: 1260–1263. doi:10.1016/S0304-4238(01)00254-0.

El-Hafedha Ould Mohamed, A.V., Daggaria, H., and Maalej, M. 2001. Analysis of several discharge rate-spacing-duration combinations in drip irrigation system. Agric. Water Manage. **52**: 33–52. doi:10.1016/ S0378-3774(01)00126-3.

Feddes, R.A., Kowalik, P.J., and Zaradny, H. 1978. Simulation of field water use and crop yield. In Simulation monographs. Pudoc, Wageningen. pp. 188–189. doi:10.1097/00010694-198 003000-00016.

Foley, J.A., Ramankutty, N., Brauman, K.A., Cassidy, E.S., Gerber, J.S., Johnston, M., et al. 2011. Solutions for a cultivated planet. Nature, **478**: 337–342. doi:10.1038/nature10452. PMID: 21993620.

Ghazouani, H., Rallo, G., Mguidiche, A., Latrech, B., Douh, B., Boujelben, A., and Provenzano, G. 2019. Assessing Hydrus-2D model to investigate the effects of different on-farm irrigation strategies on potato crop under subsurface drip irrigation. Water, **11**: 540. doi:10.3390/ w11030 540.

Goldberg, S.D., Rinot, M., and Karu, N. 1971. Effect of trickle irrigation intervals on distribution and utilization of soil moisture in a vineyard. Soil Sci. Soc. Am. J. **35**: 127–130. doi:10.2136/sssaj1971.03615995003500010037x.

Huang, X.F., Hu, B., and Ou, S.X. 2019. Effects of different drip-line layouts and dripper discharges on soil water–nitrogen distribution and spring wheat yield. Agric. Eng. **9**: 81–87. doi:SUN:NYGE.0.2019-10-017.

Kandelous, M.M., Šimůnek, J., van Genuchten, M.T., and Malek, K. 2011. Soil water content distributions between two emitters of a subsurface drip irrigation system. Soil Sci. Soc. Am. J. **75**: 488–497. doi:10.2136/sssaj2010.0181.

Kang, Y.H., Chen, M., and Wan, S.Q. 2010. Effect of drip irrigation with saline water on waxy maize (*Zea mays* L.var. Ceratina kulesh) in North China plain. Agric. Water Manage. **97**: 1303–1309. doi:10.1016/j.agwat.2010.03.006.

Karandish, F., and Šimůnek, J. 2018. An application of the water footprint assessment to optimize production of crops irrigated with saline water: a scenario assessment with HYDRUS. Agric. Water Manage. **208**: 67–82. doi:10.1016/j.agwat.2018.06.010.

Karandish, F., and Šimůnek, J. 2019. A comparison of the HYDRUS(2D/3D) and SALTMED models to investigate the influence of various water-saving irrigation strategies on the maize water footprint. Agric. Water Manage. **213**: 809–820. doi:10.1016/j.agwat. 2018.11.023.

Khosla, B.K. 1996. Agricultural salinity assessment and management. J. Indian Soc. Soil Sci. **44**: 360–360. doi:10.1061/9780784411698.

Kumar, S., Sonkar, I., Gupta, V., Hari Prasad, K.S., and Ojha, C.S.P. 2021. Effect of salinity on moisture flow and root water uptake in sandy loam soil. J. Hazard. Toxic Radioact. Waste. **25**: 04021016. doi:10.1061/(ASCE)HZ.2153-5515.0000618.

Li, D.X., Dai, X.P., Feng, J., Lei, H.J., and Cai, H.M. 2012. Effects of dripper discharges and irrigation amount on soil water movement under drip irrigation. Water Sav. Irrig. **2012**(2): 13–15.

Li, M.S., Xie, Y., and Cui, W.M. 2007. Experimental study on factors influencing soil moisture uniformity under linear source drip irrigation. J. Irrig. Drain. **6**: 11–14+33. doi:10.13522/j.cnki.ggps.2007.06.005.

Li, X., Jin, M., Zhou, N., Jiang, S., and Hu, Y. 2018. Inter-dripper variation of soil water and salt in a mulched drip irrigated cotton field: advantages of 3-D modelling. Soil Tillage Res. **184**: 186–194. doi:10.1016/j.still.2018.07.016.

Li., X.B., Kang, Y.H., Wan, S.Q., Chen, X.L., and Chu, L.L. 2015. Reclamation of very heavy coastal saline soil using drip-irrigation with saline water on salt-sensitive plants. Soil Tillage Res. **14**: 6159–6173. doi:10.1016/j.still.2014.10.005.

Ma, M.M., Lin, Q., and Xu, S.H. 2020. Water infiltration characteristics of layered soil under influences of different factors and estimation of hydraulic parameters. Acta Pedologica Sinica, **57**: 347–358. doi:10.11766/trxb201905090250.

Meng, Z.J., Bian, X.M., Pang, H.B., and Wang, H.Z. 2008. Effect of regulated deficit irrigation on growth and development characteristics in cotton and its yield and fiber quality. Cotton Sci. **1**: 39–44. doi:10.3969/j.issn.1002-7807.2008.01.008

Mizrahi, Y., Taleisnik, E., Kagan-Zur, V., Zohar, Y., Offenbach, R., Matan, E., and Golan, R. 1988. A saline irrigation regime for improving tomato fruit quality without reducing yield. J. Am. Soc. Hort. Sci. **113**: 202–205. doi:10.21273/JASHS.113.2.202.

Nazari, E., Besharat, S., Zeinalzadeh, K., and Mohammadi, A. 2020. Measurement and simulation of the water flow and root uptake in soil under subsurface drip irrigation of apple tree. Iran. J. Irrig. Drain. **13**: 1806–1809. doi:10.1016/j.agwat.2021.106972.

Niu, W.Q., Fan, X.K., Zhou, X.B., and Chen, J.Y. 2012. Effect of initial water content on soil infiltration characteristics during bubble irrigation. J. Drain. Irrig. Machin. Eng. **30**: 491–496. doi:10.3969/j.issn.1674-8530.2012.04.022.

Rahneshan, Z., Nasibi, F., and Moghadam, A.A. 2018. Effects of salinity stress on some growth, physiological, biochemical parameters and nutrients in two pistachio (*Pistacia vera* L.) rootstocks. J. Plant Interact. **13**: 73–82. doi:10.1080/17429145. 2018.1424355.

Rasouli, F., Pouya, A.K., and Šimůnek, J. 2013. Modeling the effects of saline water use in wheat-cultivated lands using the UNSATCHEM model. Irrig. Sci. **31**: 1009–1024. doi:10.1016/j.agwat.2020.106601.

Santhi, C., Arnold, J.G., Williams, J.R., Dugas, W.A., Srinivasan, R., and Hauck, L.M. 2001. Validation of the SWAT model on a large river basin with point and nonpoint sources. J. Am. Water Resour. Assoc. **37**: 1169–1188. doi:10.1111/j.1752-1688. 2001.tb 03630.x.

Shiri, J., Karimi, B., Karimi, N., Kazemi, M.H., and Karimi, S. 2020. Simulating wetting front dimensions of drip irrigation systems: multi criteria assessment of soft computing models. J. Hydrol. **585**: 124792. doi:10.1016/j.jhydrol.2020.124792.

Šimůnek, J., van Genuchten, M.T., and Šejna, M. 2016. Recent developments and applications of the HYDRUS computer software packages. Vadose Zone J. **15**: 1539–1663. doi:10.2136/vzj2016.04.0033.vzj2016.04.0033.

Srinet, R., Nandy, S., and Patel, N.R. 2019. Estimating leaf area index and light extinction coefficient using Random Forest regression algorithm in a tropical moist deciduous forest, India. Ecological Informatics. **52**: 94–102. doi:10.1016/j.ecoinf.2019.05.008.

Stein, E.V., Emily, G., and Chun, W.Y. 2020. Fertility, mortality, migration, and population scenarios for 195 countries and territories from 2017 to 2100: a forecasting analysis for the global burden of disease study. Lancet, **396**: 1285–1306. doi:10.1016/S0140-6736(20) 30677-2.

Wan, S.Q., Kang, Y.H., Wang, D., and Liu, S.P. 2010. Effect of saline water on cucumber (*Cucumis sativus* L.) yield and water use under drip irrigation in North China. Agric. Water Manage. **98**: 105–113. doi:10.1016/j.agwat.2010.08.003.

Wang, Z.M., Jin, M.G., Šimůnek, J., and van Genuchten, T. 2012. Evaluation of mulched drip irrigation for cotton in arid northwest China. Irrig. Sci. **32**: 15–27. doi:10.1007/s0 0271-013-0409-x.

Water Resource Bulletin, 1998. People's Daily Newspaper, 4th ed. China Water Press, Beijing, China.

Yang, G., Li, F.D., Tian, L.J., He, X.X., Li, Y. Gao, Y.L., et al. 2020. Soil physicochemical properties and cotton (*Gossypium hirsutum* L.) yield under brackish water mulched drip irrigation. Soil Tillage Res. **199**: 104592. doi:10.1016/j.still.2020.104592.

Yin, Q.R., Zhang, X.C., and Wang, D.D. 2011. Effect of initial water content on saturated hydraulic conductivity and salt leaching of alkaline soil. Bull. Soil Water Conserv. **31**: 71–74. http://ir.iswc.ac.cn/handle/361005/5072.

Yuan, C.F., Feng, S.Y., Huo, Z.L., and Ji, Q.Y. 2019. Simulation of saline water irrigation for seed maize in arid northwest China based on SWAP model. Sustainability, **11**: 4264. doi:10. 3390/su 11164264.

Zeng, C., Wang, Q.J., and Fan, J. 2010. Effect of initial water content on vertical line-source infiltration characteristic of soil. Trans. CSAE, **26**: 24–30. doi:10.3969/j.issn. 1002-6 819.2010.01.005.

Zhang, Y.H., Li, X.Y., Šimůnek, J., Shi, H.B., Chen, N., Hu, Q., and Tian, T. 2021. Evaluating soil salt dynamics in a field drip-irrigated with brackish water and leached with freshwater during different crop growth stages. Agric. Water Manage. **244**: 106601. doi:10.1016/j.agwat.2020.106601.